Organic Electronics 13 (2012) 2620–2626

Contents lists available at SciVerse ScienceDirect

Organic Electronics

journal homepage: www.elsevier.com/locate/orgel

A study of bulk current mechanism in P3HT-based thin film transistors and approach for current suppression

Chia-Hao Chang [a], Chao-Hsin Chien [a,b,*]

[a] Department of Electronics Engineering and Institute of Electronics, National Chiao Tung University, Hsinchu, Taiwan, ROC
[b] National Nano Device Laboratories, Hsinchu, Taiwan, ROC

ARTICLE INFO

Article history:
Received 27 February 2012
Received in revised form 12 June 2012
Accepted 25 June 2012
Available online 2 August 2012

Keywords:
P3HT
OTFTs
Polymer semiconductor
Bulk current effect
Electrodes
MWCNTs

ABSTRACT

In this article, poly(3-hexylthiophene) (P3HT) based thin film transistors with Ti capped source and drain electrodes (S/D) was employed to have an insight into the mechanism of bulk current effect, which led to poor subthreshold swing and large off current. Our newly developed PTFTs do show greater characteristics in the aspects of on/off current ratio and subthreshold swing than those with the conventional Au/Ti S/D. In order to explain the results, we propose that the bulk current is composed of two components, i.e., side-wall and top-face injections. We ascribe the improvements to the reduction of top-face injection bulk current due to the larger injection barrier between the P3HT and Ti. As comparing the PTFTs with Ti capped laterally grown multi-wall carbon nanotube (MWCNT) S/D with the PTFTs with MWCNT S/D, we also observe similar tendency of bulk current reduction. From the viewpoint of device operation, better subthreshold swing and smaller off current result in faster device switching and lower power consumption. By this new approach of S/D structure, there are two and 20 times improvements on the subthreshold swing and off current, respectively, although the reduction of the bulk current also leads to a slight decrease of the on-current.

1. Introduction

Organic semiconductors, such as polymers, are attractive since they have the potential to be easily applied on a large scale flexible substrate due to the fact that the required process temperature is pretty low. Solution processable, self-organized, regioregular poly(3-hexylthiophene) (P3HT) is very suitable to the fabrication of organic thin film transistors (OTFTs) since theses transistors demonstrate relatively high carrier mobility. The hole mobility of OTFTs with a P3HT active layer (i.e., PTFTs) have been demonstrated as high (0.01–0.3 $cm^2/V\,s$) as amorphous silicon thin film transistors with a reasonable on/off ratio (more than 100 in air and 10^6 in an inert atmosphere) [1–5]. However, the performance of PTFTs can be significantly influenced by the channel coating method and the macromolecular parameters of channel material [1,3–5]. The electrical properties can be improved by incorporating surface treatment on the surface of gate and electrodes, and post treatments such as O_2 plasma treatment and thermal annealing [3,4,6,7]. Recently, many researchers have proposed that the characteristics of PTFTs were correlative to the thickness of active layer [8–10]. This effect was attributed to the existence of bulk current in the active layer before the formation of accumulation layer, and, usually, higher bulk current would be conducted in a thicker active layer [8,9]. Moreover, poor off-current and subthreshold swing were observed when the thickness of active layer was increased [8–10]. This topic has been getting more and more attention, and different methods

* Corresponding author. Address: Electronics Engineering and Institute of Electronics, National Chiao-Tung University, 1001 University Road, Hsinchu 300, Taiwan, ROC. Tel.: +886 3 5712121x54252; fax: +886 3 5724361.
E-mail address: chchien@faculty.nctu.edu.tw (C.-H. Chien).

1566-1199/$ - see front matter © 2012 Elsevier B.V. All rights reserved.
http://dx.doi.org/10.1016/j.orgel.2012.06.042

have proposed by different groups [10–13]. However, the detailed studies on the mechanism of bulk current and the method to suppress it are still lack.

In this study, PTFTs with Ti capped source and drain electrodes (S/D), formed by coating a Ti layer on conventional Au/Ti S/D, were employed to study the bulk current effect. By comparing the results of PTFTs with conventional Au/Ti and Ti capped S/D, the improvements on the subthreshold swing and the on/off current ratio for PTFTs with Ti capped S/D are clearly observed. We attribute this result to the reduction of top-face injected bulk current. We find that there is more than one order of magnitude of reduction in the off-current level, as well as an obviously increased on/off current ratio, and a much lower subthreshold swing as PTFTs with thin P3HT layer. With the systematic studies, we have an insight on the origin of the effects coming from the bulk current of PTFTs and provide an approach to suppress this leakage current. Moreover, we also observe similar tendency of bulk current reduction when comparing the PTFTs with Ti capped laterally grown multi-wall carbon nanotube (MWCNT) S/D with those with MWCNT S/D.

2. Experimental procedure

Fig. 1 depicts the schematic cross section of PTFTs. The speculated components of bulk current injected from the different source electrodes in subthreshold region for PTFTs with conventional and Ti capped Au/Ti S/D are shown in Fig. 1a and b, respectively. We will address current components in detail later. The N^{++} doped silicon substrate and thermally grown oxides of 200 nm thickness were used as gate electrodes and insulators, and then a lift-off process patterned Au/Ti (50 nm/2.5 nm) or Ti (10 nm) capped Au/Ti (50 nm/2.5 nm) were deposited by an electron beam thermal evaporation as the source/drain. Moreover, PTFTs with MWCNT S/D or Ti capped laterally grown MWCNT S/D were also employed. For MWCNT S/D formation, a Fe/Ti catalytic and buffer layer was deposited and patterned through electron beam thermal evaporation and the lift-off technique on gate insulator, producing thicknesses of 5 nm and 10 nm for the Fe and Ti layer, respectively. Subsequently, the MWCNTs were grown through thermal CVD using the following procedure: the samples were heated to 700 °C in a nitrogen gas atmosphere. After pretreatment of the Fe/Ti catalytic layer in a mixed gas flow of hydrogen and nitrogen, conventionally, MWCNTs were vertically grown on the S/D region through pyrolysis of ethylene (C_2H_4), used as the carbon source, over a growth time of 10 min. For Ti capped laterally grown MWCNT S/D formation, a Ti (10 nm) capped Fe/Ti (5 nm/10 nm) was used and went through the same processes as MWCNT S/D formation, and the MWCNTs were intentionally grown on the side-wall of the electrodes, i.e., laterally grown MWCNTs, from the exposed Fe particles. Some article had demonstrated methods to laterally grow MWCNTs [14,15]. Fig. 2a and b depict the schematic cross sections of PTFTs with MWCNT S/D and Ti capped laterally grown MWCNT S/D. Prior to the deposition of P3HT as the channel, the substrate was cleaned by acetone, isopropyl alcohol and deionized (DI) water in an ultrasonic bath for 5 min, respectively, and treated by hexamethyl disilazane (HMDS) passivation in a vacuum oven at 150 °C to create a hydrophobic surface. Then, the P3HT active layer was spun in yellow bay using a two-step process—1000 rpm for 10 s in the first step and 1500 rpm for 25 s in the second step, followed by baking at 150 °C for 3 min. Chloroform was used as the solvent for P3HT,

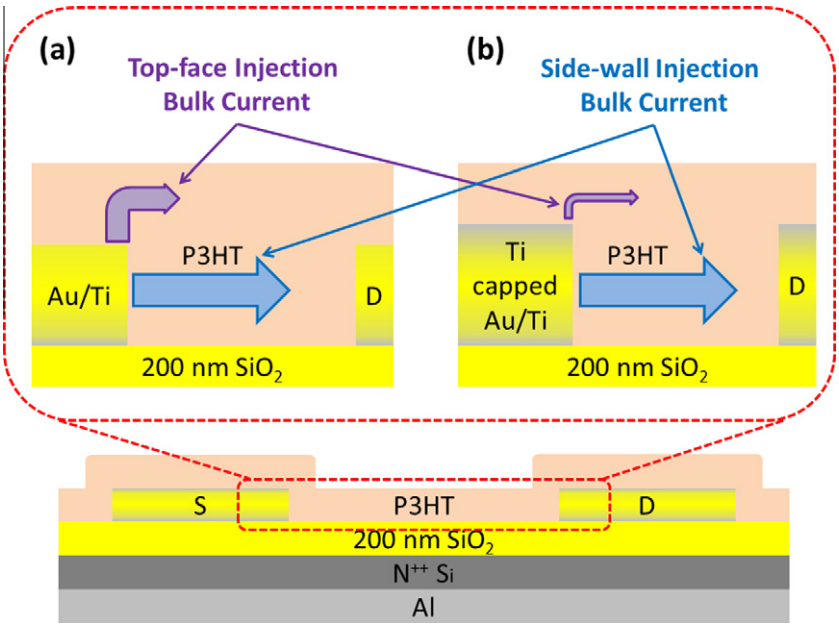

Fig. 1. A schematic cross section of PTFTs is depicted, and the components of bulk current injected from different source electrodes under subthreshold region for PTFTs with conventional and Ti capped Au/Ti S/D are shown in (a) and (b), respectively.

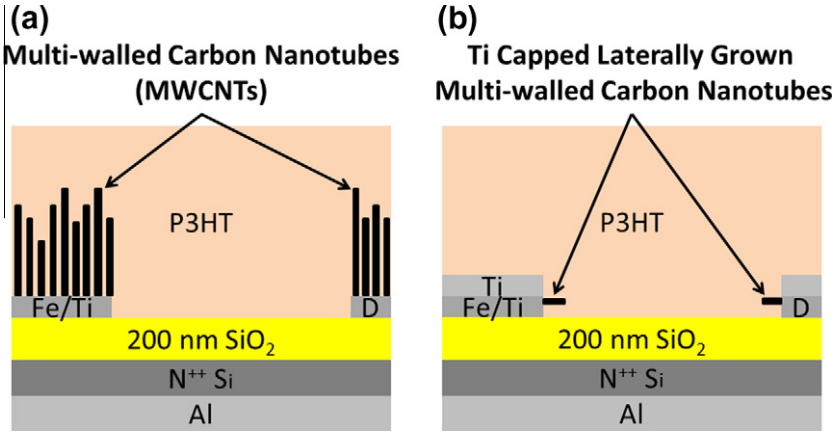

Fig. 2. Schematic cross sections of PTFTs is depicted, and PTFTs with MWCNT and Ti capped laterally grown MWCNT S/D are shown in (a) and (b), respectively.

resulting in a weight percentage of solutions for P3HT in chloroform of 0.05 and 0.2 wt.%. All of the P3HT solutions were treated with ultrasonic vibration for 5 min before usage and were percolated by a PTFE membrane syringe filter with a pore size of 0.2 μm. The regioregular P3HT used in this study was purchased from FEM Inc. (Mw = 50000), and the provided coupling ratio of head–tail to head–head and tail–tail was approximately 90%. The top views of PTFTs with MWCNT S/D and Ti capped laterally grown MWCNT S/D were observed by using optical microscope (OM). The electrical properties of P3HT TFTs were measured by a Hewlett–Packard 4156C semiconductor parameter analyzer, and the devices were evaluated at their saturation region with a drain voltage of −60 V. We extracted mobility by maximum transconductance in the saturation region. All of the devices were processed and characterized in air atmosphere.

3. Results and discussion

The drain current–gate voltage (I_D–V_G) characteristics of the fabricated PTFTs with conventional and Ti capped S/D are shown in Fig. 3. The employed weight percentages of solutions of P3HT in chloroform were 0.05 and 0.2 wt.%. By comparing the results of the PTFTs with conventional S/D with different channel thicknesses, we find the PTFTs with thick active layer coated with 0.2 wt.% solution exhibit poorer off current and subthreshold swing than those with thin active layer coated with 0.05 wt.% solution. We think that this result might be closely related to the presence of bulk current [8,9]. This early conduction increases with the raising thickness because of the decrease in the channel resistance. Larger the early conduction, i.e., bulk current, more positive threshold voltage shift is. Moreover, since the channel resistance varies with the gate bias that inducing band bending of active layer before the accumulation layer formation, the bulk current will increase with increasing negative gate voltage bias and then also contribute to the on-current. As a result, in order to have a superior switching performance, this bulk current shall be avoided as far as possible. The goal can be attained by using asymmetric electrodes or incorporating an insulating mesa-like structure in between source and drain electrodes [11–13]. However, these processes obviously are not consistent with low cost and easy process.

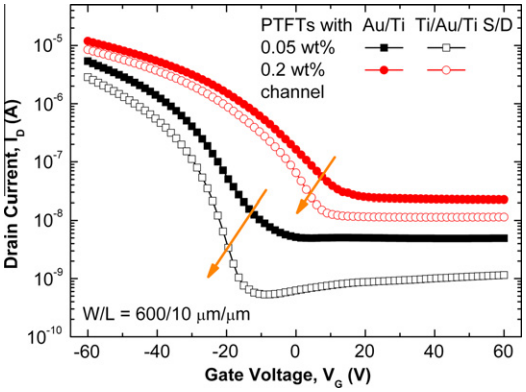

Fig. 3. Transfer current characteristics of PTFTs with Au/Ti and Ti capped Au/Ti S/D, and different P3HT thicknesses, which are coated by 0.05 and 0.2 wt.% solution.

Jung et al. had proposed that the carrier injection into the accumulated channel was via two possible paths, i.e., top-face and side-wall injections [16]. By two dimensional numerical simulation and analytical model, Islam demonstrated that the subthreshold performance of the devices with a stack contact (A electrode structure composed by a low work function metal upper layer and a high work function metal under layer.) could be significantly improved [10]. Nevertheless, unfortunately, the detail of mechanism of bulk current is still insufficient because the device structure used in his simulation is not similar to the typical device structure in which both the surface of gate insulator and electrodes are covered with the channel layer [10]. Inspired by the proposal of Jung et al. and based on the properties of PTFTs with Au/Ti S/D, we suppose that the bulk current might also consist of two injection current paths, i.e., top-face and side-wall injections, as shown in Fig. 1a. In an aim to verify our inference, we

incorporated a layer of Ti upon the conventional S/D and find that the performance of the PTFTs dramatically changes accompanying with the introduction of Ti capping, as shown in Fig. 3. The device obviously shows sharper subthreshold region and lower off-current level. Moreover, the impact of Ti introduction becomes more conspicuous when there is a thin P3HT layer. This result implies that the side-wall injected bulk current becomes dominant over the top-face injected current when the channel thickness was increased. However, with comparison of PTFTs with Au/Ti and Ti capped Au/Ti S/D, the larger injection barrier between Ti and the P3HT causes the reduction of top-face injected bulk current, as shown in Fig. 1b, and in turn results in lower off-current level and better subthreshold swing. It should be noticed that PTFTs with Ti (50 nm) S/D, i.e., without employing Au, exhibit almost no current flow in the accumulation layer, which is not shown here. For the PTFTs with thin active layer, the mobility is 0.008 cm^2/Vs (0.006 cm^2/Vs) for PTFTs with Au/Ti S/D (PTFTs with Ti capped Au/Ti S/D), comparable to the values shown in the recent literatures [6,7]. In addition, the on/off current ratio and subthreshold swing were improved from 1.1×10^3 and 9.85 V/decade for PTFTs with Au/Ti S/D to 5.4×10^3 and 5.3 V/decade for PTFTs with Ti capped Au/Ti S/D. The improvement cannot be predicted by the well-known formula for on/off current ratio [17,18]. It also cannot be explained by the space-charge limited current (SCLC) model, which is in common used to explain the bulk current effect [8,10].

The drain current–drain voltage (I_D–V_D) characteristics under a gate voltage bias of 0 V are shown in Fig. 4. The performances of PTFTs with different P3HT thicknesses, which were coated by 0.2 and 0.05 wt.% solution, are shown in Fig. 4a and b, respectively. There might be no issue on the drain current which is fully composed of the bulk current as the gate voltage is of 0 V, and this current usually is regarded as the leakage current. Obviously, the drain current of PTFTs with Ti capped Au/Ti S/D are lower than that of the PTFTs with conventional S/D. Especially, for PTFTs using thin channel layer, the drain current is dramatically reduced, as shown in Fig. 4b. There is a 20 fold decrease on the drain current or bulk current. However, for PTFTs with thick channel layer, the drain current exhibits only twofold reduction, as shown in Fig. 4a. Although the effect of reducing top-face injection bulk current is still observable for the PTFTs with thick channel layer, the current mainly leaks through the side-wall of electrodes. This means that the side-wall injection dominates over top-face injection. Comparatively, for PTFTs with thin channel layer, side-wall injection is suppressed by the thinner channel layer due to the higher channel resistance so that the top-injection becomes more important. The effect of reducing bulk current induced by suppressing top-face injection part by the Ti capping layer is more conspicuous. These results again are consistent to our interpretations.

As shown in Fig. 5, we extracted the values of the contact and channel resistances of the samples in Fig. 3 by transmission line method (TLM). The values of contact resistance of both PTFTs with Au/Ti S/D and with different channel thicknesses are close to 2×10^9 Ω-μm. This represents the coverage of P3HT on the channel and S/D region was still pretty well when thin channel was used. Therefore, the possibility that different P3HT thicknesses lead to different performances, shown in Fig. 3, due to the distinct coverage of P3HT can be excluded. As we have mentioned, the larger side-wall injected bulk current due to the thicker P3HT layer is responsible for the resultant lower channel resistance. Furthermore, while the S/D was replaced by Ti capped Au/Ti, the contact resistance only slightly increases from 2×10^9 to 6×10^9 Ω-μm or from 1.5×10^9 to 2.0×10^9 Ω-μm for PTFTs with thin or thick active layer, respectively. The increase is thought to be correlated to the suppression of top-face injected bulk current and only weight a small portion of contact resistance. As a result, we think our argument that the side-wall injected bulk current is the dominant current component for the

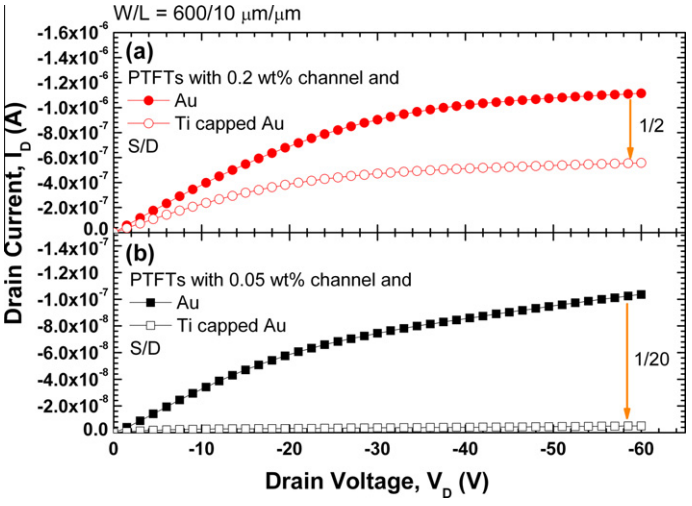

Fig. 4. Drain current–drain voltage (I_D–V_D) characteristics of PTFTs with Au/Ti and Ti capped Au/Ti S/D under a gate voltage bias of 0 V. The performances of PTFTs with different thicknesses of P3HT layers coated by 0.2 and 0.05 wt.% solution are shown in (a) and (b), respectively.

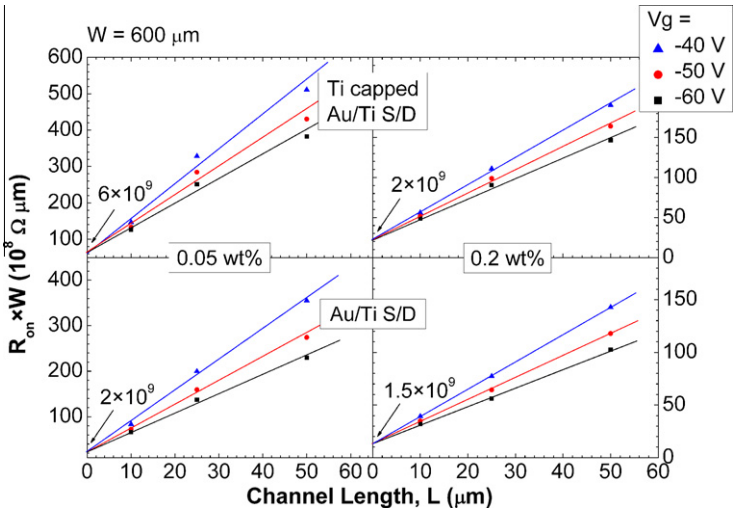

Fig. 5. The results of contact and channel resistance correlated to the samples in Fig. 3, which were extracted by transmission line method (TLM).

Table 1
Summation of the parameters for the PTFTs with different thicknesses, and Au/Ti or Ti capped Au/Ti S/D.

Samples, PTFTs with	μ_{fet} (cm^2/Vs)	S.S. (V/dec.)	V_t (V)	I_{on}/I_{off}
0.05 wt.% Channel and Au/Ti S/D	0.00884	9.85	−22	1.1×10^3
0.2 wt.% Channel and Au/Ti S/D	0.00803	15.7	−3	5.26×10^2
0.05 wt.% Channel and Ti capped Au/Ti S/D	0.00609	5.30	−25	5.39×10^3
0.2 wt.% Channel and Ti capped Au/Ti S/D	0.00607	10.2	−4	7.5×10^2

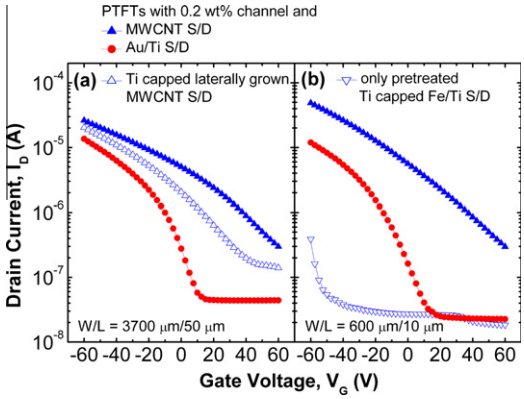

Fig. 6. (a) Transfer current characteristics of PTFTs with MWCNT S/D and Ti capped laterally grown MWCNT S/D. (b) Transfer current characteristics of PTFTs with vertical MWCNT S/D and no laterally grown MWCNT S/D. In other words, only pretreatment was performed. P3HT was coated with 0.2 wt.% solution, and the transfer curves of PTFTs with Au/Ti S/D are also incorporated for comparison.

PTFTs with thick active layer is rather plausible, and the result is consistent with the conspicuous performance improvement resulted from suppressing top-face injection bulk current for PTFTs with thin active layer. The parameters of all PTFTs with thin and thick P3HT layer with Au/Ti and Ti capped Au/Ti S/D are summarized in Table 1.

This effect of reducing bulk current by incorporating a layer of Ti upon the electrodes shall still be observable when the electrode material is changed. We therefore replaced Au by MWCNTs since we had demonstrated that pentacene and P3HT based TFTs showed superior performance by employing MWCNTs as the electrodes [19,20]. We obtained the increased on-current and reduced contact resistance. However, it is anticipated that there will be a larger bulk current, i.e., easier early conduction, because of the reduced contact resistance. The drain current–gate voltage (I_D–V_G) characteristics of the fabricated PTFTs with MWCNT S/D or Ti capped laterally grown MWCNT S/D are shown in Fig. 6a. The performance of PTFTs with Au/Ti S/D is also shown as the control. The employed weight percentage of solution of P3HT in chloroform was 0.2 wt.%. As shown in Fig. 6a, both the PTFTs with MWCNT and Ti capped laterally grown MWCNT S/D have the benefits resulting from employing MWCNT S/D and, as expected, larger bulk current than the PTFTs with Au/Ti S/D is also observed. However, obviously, the improvements on the subthreshold swing and off-current by incorporating Ti capping layer are still observed. Moreover, the performance of PTFTs with Ti capped directly on Fe/Ti layer without MWCNT growth is shown in Fig. 6b. For comparison, the performance of PTFTs with MWCNT S/D and Au/Ti S/D is also incorporated. Obviously, if there was no MWCNTs grew on the side-wall of electrode, i.e., no laterally grown MWCNTs, no current could conduct in the P3HT layer because of high injection barrier even the gate voltage bias is high enough to form the accumulation layer. This result could exclude the doubt about that the drain current of PTFTs with Ti capped laterally grown MWCNT S/D might not come from laterally grown MWCNTs but the pretreated Ti capped Fe/Ti.

In addition, there might be concern that the effective channel length was reduced due to the laterally grown

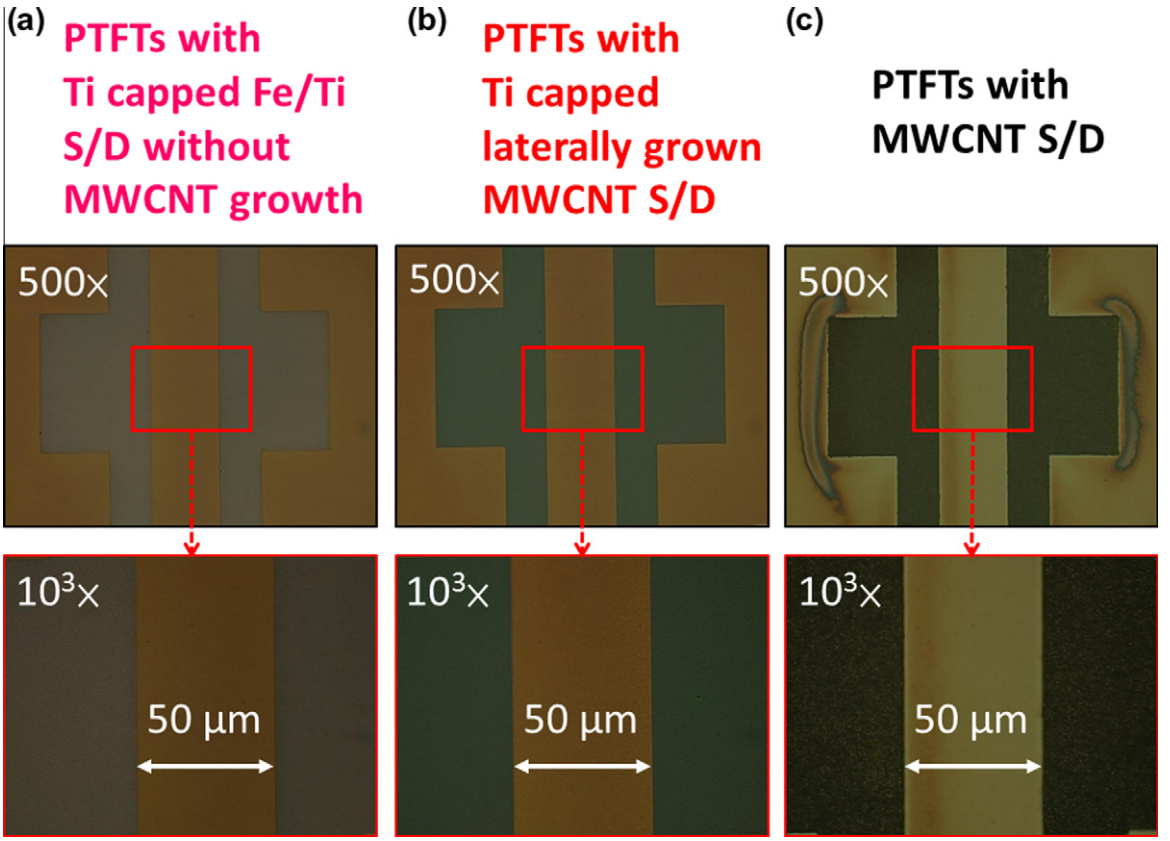

Fig. 7. Optical micrographs of the PTFTs with different electrodes, (a) Ti capped Fe/Ti S/D without MWNCT growth, (b) Ti capped laterally grown MWCNT S/D, and (c) vertical grown MWCNT S/D.

MWCNTs. Hence to confirm the length of laterally grown MWCNTs is needed. However, we failed to directly confirm the laterally grown MWCNTs by using scanning electron microscope (SEM) because of the fact that there was the magnetic interference induced by Fe. As an alternative, the top views of the PTFTs with different electrodes were observed by using OM as shown in Fig. 7. The channel region of the PTFTs with Ti capped laterally grown MWCNT S/D (Fig. 7b) was similar to that of the PTFTs with Ti capped Fe/Ti S/D without MWCNT growth (Fig. 7a). In other words, if the length of the laterally grown MWCNTs is sufficient to influence the channel length, the edges of the Ti capped electrodes would be as black as the vertical grown MWCNTs (Fig. 7c). Therefore, we infer that the length of laterally grown MWCNTs is so short such that the influence on the channel length can be ignored. Supposedly, the short length might be due to the thin catalytic layer (5 nm), resulting in a small exposure area for carbon source and slower MWCNT growth rate. Accordingly, the doubt about the influence of carbon nanotubes on the channel length can be excluded. Moreover, someone may suspect that we have failed to grow the laterally grown MWCNTs. Instead of that, there might be carbide formation and, in turn, lead to the improvement in mobility. This doubt could be excluded because of the fact that the work function of Ti–C and Fe–C are ~4 eV and ~4.5 eV, respectively [21,22]. Clearly, relatively large carrier injection barrier will be induced, which does not benefit the performance if the carbides were really formed. Thus, the laterally grown MWCNTs do exist and contribute to the improvement in the on-current level.

4. Conclusion

In this paper, we present an insight into the bulk current effect of PTFTs, and provide an approach to suppress it. The bulk current was composed of side-wall and top-face injection currents. With proper scheme, bulk current could be significantly reduced and enhance the performance of PTFTs. Our newly developed PTFTs with a modified structure by employing a Ti capping Au/Ti S/D did show the improvements on subthreshold swing and on/off current ratio. We think that these improvements mainly come from the reduction of top-face injected bulk current. For the PTFTs with thin active layer, there is greater than one order of magnitude of reduction in the off-current level, as well as an obviously increased on/off current ratio, and a much lower subthreshold swing. Furthermore, we fabricated the novel PTFTs which used a Ti capped laterally grown MWCNTs as the electrodes to strengthen the foundation of our inference. With the evidence provided by

the newly developed transistors, we find our approach to suppress the bulk current is effective and useful.

References

[1] H. Sirringhaus, P.J. Brown, R.H. Friend, M.M. Nielsen, K. Bechgaard, B.M.W. Langeveld-Voss, A.J.H. Spiering, R.A.J. Janssen, E.W. Meijer, P. Herwig, D.M. de Leeuw, Nature 401 (1999) 685.
[2] H. Sirringhaus, N. Tessler, R.H. Friend, Science 280 (1998) 1741.
[3] G. Wang, J. Swensen, D. Moses, A.J. Heeger, J. Appl. Phys. 93 (2003) 6137.
[4] S. Cho, K. Lee, J. Yuen, G. Wang, D. Moses, A.J. Heeger, M. Surin, R. Lazzaroni, J. Appl. Phys. 100 (2006) 114503.
[5] H. Yang, T.J. Shin, Z. Bao, C.Y. Ryu, J. Polym. Sci. Part B: Polym. Phys. 45 (2007) 1303.
[6] S.K. Park, Y.H. Kim, J.I. Han, D.G. Moon, W.K. Kim, IEEE Trans. Elect. Dev. 49 (2002) 2008.
[7] S.K. Park, Y.H. Kim, J.I. Han, D.G. Moon, W.K. Kim, M.G. Kwak, Synth. Met. 139 (2003) 377.
[8] M.J. Deen, M.H. Kazemeini, Y.M. Haddara, J. Yu, G. Vamvounis, S. Holdcroft, W. Woods, IEEE Trans. Elect. Dev. 51 (2004) 1892.
[9] E. von Hauff, F. Johnen, A.V. Tunc, L. Govor, J. Parisi, J. Appl. Phys. 108 (2010) 063709.
[10] M. Nurul Islam, J. Appl. Phys. 110 (2011) 114906.
[11] M.H. Lim, I.Y. Lee, S.G. Jeong, J. Lee, W.S. Jung, H.Y. Yu, G.H. Kim, Y. Roh, J.H. Park, Org. Electron. 13 (2012) 1056.
[12] W.Y. Chou, S.T. Lin, H.L. Cheng, F.C. Tang, Y.J. Lin, C.F. You, Y.W. Wang, Appl. Phys. Lett. 90 (2007) 222103.
[13] J.Z. Wang, Z.H. Zheng, H. Sirringhaus, Appl. Phys. Lett. 89 (2006) 083513.
[14] Y.S. Han, J.K. Shin, S.T. Kim, J. Appl. Phys. 90 (2001) 5731.
[15] B.H. Chen, P.Y. Lo, J.H. Wei, M.J. Tsai, C.L. Hwang, T.S. Chao, H.C. Lin, T.Y. Huang, Electrochem. Solid-State Lett. 8 (2005) G290.
[16] K.D. Jung, Y.C. Kim, H. Shin, B.G. Park, J.D. Lee, E.S. Cho, S.J. Kwon, Appl. Phys. Lett. 96 (2010) 103305.
[17] A.R. Brown, C.P. Jarrett, D.M. de Leeuw, M. Matters, Synth. Met. 88 (1997) 37.
[18] G. Horowitz, Adv. Mater. 10 (1998) 365.
[19] C.H. Chang, C.H. Chien, J.Y. Yang, Appl. Phys. Lett. 91 (2007) 083502.
[20] C.H. Chang, C.H. Chien, IEEE Electron Device Lett. 32 (2011) 1457.
[21] F. Santerre, M.A. El Khakani, M. Chaker, J.P. Dodelet, Appl. Surf. Sci. 148 (1999) 24.
[22] X. Tan, J. Zhou, F. Liu, Y. Peng, B. Zhao, Eur. Phys. J. B 74 (2010) 555.